RSC Advances

ROYAL SOCIETY OF CHEMISTRY

PAPER

View Article Online
View Journal | View Issue

Cite this: *RSC Adv.*, 2026, **16**, 25040

Influence of solvent effect, temperature, and pressure on the aggregation behavior of island model asphaltene: a molecular dynamics study

Cun Hu, *[abc] Dandan Hong,[abc] E. Fu,[abc] Yalou Sun,[abc] Jipeng Wang,[abc] Li Chen,[a] Xiaoyu Hu,[abc] Jun Wang,[abc] Zhaohui Hu,[abc] Wenjing Shi,[abc] Zhi Cao,[abc] Changchun Wang[abc] and Lulu Hu*[abc]

Received 6th January 2026
Accepted 5th May 2026

DOI: 10.1039/d6ra00135a

rsc.li/rsc-advances

The aggregation of asphaltene molecules strongly affects crude oil stability and flow assurance, yet the microscopic mechanisms remain unclear. In this study, molecular dynamics simulations were performed on the representative island-type asphaltene to investigate the effects of solvent composition, temperature, and pressure on its aggregation behavior. Thermodynamic and structural analyses were conducted using total energy, solvent accessible surface area (SASA), and intermolecular hydrogen bonding. Results show that solvent composition is the dominant factor: low toluene fractions (≤30%) enhance van der Waals interactions and promote compact aggregates, while higher toluene contents increase solvation and suppress aggregation. Temperature exhibits a nonlinear influence – moderate temperatures (60–70 °C) yield the lowest energy and most stable aggregates, whereas excessive or insufficient thermal motion at high or low temperatures weakens aggregation. Pressure has a secondary but notable effect: at moderate pressure (∼2 MPa), aggregates become looser due to enhanced solvation, while both low and high pressures favor denser, more stable configurations. Overall, asphaltene aggregation is jointly controlled by solvent polarity, temperature, and pressure, providing molecular-level insights for predicting and mitigating asphaltene deposition in petroleum systems.

1. Introduction

Asphaltenes are among the most complex and problematic components of crude oil, and their aggregation and deposition behaviors significantly affect crude oil flowability, reservoir permeability, and the operational stability of production systems.[1–6] The aggregation of asphaltenes is a multiscale, stepwise process driven by intermolecular forces such as π–π stacking, hydrogen bonding, and van der Waals interactions, while being strongly modulated by environmental factors including solvent properties, temperature, and pressure.[7–11] During oil production and transportation, variations in thermodynamic conditions alter asphaltene solubility and stability, leading to molecular aggregation, flocculation, and eventual deposition in the wellbore, pipelines, and reservoir pores.[7,12,13] Such processes can cause severe plugging, production decline, and equipment corrosion, making it essential to elucidate the molecular mechanisms and environmental responses of asphaltene aggregation.

Molecular dynamics (MD) simulation has become an important tool to investigate the behavior of asphaltenes.[14,15] Two principal structural models have been proposed to describe asphaltene molecular architecture: the island and archipelago models.[16–18] In the island model, a single large polyaromatic core is surrounded by alkyl side chains or polar substituents, and aggregation is primarily driven by π–π stacking between aromatic rings, assisted by secondary van der Waals and hydrogen bonding interactions.[19] These molecules often self-assemble into ordered lamellar or columnar structures that are more stable in nonpolar solvents (*e.g.*, *n*-heptane) but become dispersed in polar solvents (*e.g.*, toluene). Conversely, archipelago-type asphaltenes consist of several smaller aromatic units linked by aliphatic bridges or heteroatom bonds.[17,20–22] Their aggregation is governed mainly by hydrogen bonding and solvent–solute interactions, making them more environmentally sensitive. Spectroscopic and molecular simulation studies indicate that naturally occurring asphaltenes more closely resemble the island model, whose strong π–π stacking interactions and low solubility are primarily responsible for deposition and flow-assurance challenges.[23,24]

Environmental conditions play a decisive role in governing asphaltene aggregation. Temperature affects both molecular

---

[a] *The 404 Company Limited, China National Nuclear Corporation, Jiayuguan 735100, China*

[b] *Key Laboratory of Nuclear Fuel Cycle Technology, The 404 Company Limited, China National Nuclear Corporation, Jiayuguan 735100, China*

[c] *Chengdu Nuclear Engineering Design & Research Institute Co., Ltd, 404., CNNC, Chengdu, 610000, China. E-mail: hucun402@163.com; L_L_Hu@163.com*

motion and solvent polarity: increasing temperature weakens π–π stacking and hydrogen bonds, promoting dispersion, whereas cooling enhances molecular association and precipitation.[25,26] Pressure modifies solvent density and intermolecular spacing; higher pressures improve solvent capability and stabilize dispersed states, while pressure reduction leads to light-component volatilization and asphaltene instability.[27,28] Solvent polarity is arguably the most critical factor-polar solvents (such as toluene or alcohols) interact favorably with asphaltene polar sites, enhancing solubility, whereas nonpolar solvents (like *n*-heptane) promote molecular self-assembly and flocculation.[29,30] Beyond these, dissolved gases (*e.g.*, methane, CO_2) alter fluid density and polarity, indirectly influencing asphaltene stability; shear fields can disrupt aggregate structures; and mineral surface interactions affect adhesion and wettability, further promoting deposition.[5,31,32] Collectively, these factors highlight that asphaltene aggregation is a complex, coupled phenomenon that demands systematic investigation of its thermodynamic and solvent-dependent behavior.

In this work, molecular dynamics (MD) simulations were employed to investigate the combined effects of solvent environment, temperature, and pressure on the aggregation behavior of a representative island-type asphaltene molecule. Various toluene–*n*-heptane solvent mixtures and thermodynamic conditions were modeled to explore how intermolecular interactions, aggregate structures, and stability evolve with environmental variations. The findings provide molecular-level insights into the environmental response mechanisms of asphaltene aggregation and offer theoretical guidance for flow assurance and deposition control in complex petroleum systems.

2. Methods

2.1 Molecular models and force fields

The asphaltene molecular model employed in this study was based on the representative island-type structure reported in previous literature.[19] The detailed 2D structural diagram of the asphaltene molecular model used in this study was included in the Supplementary material (Fig. S1). *N*-Heptane was used as the poor solvent for asphaltene, whereas toluene acted as the good solvent due to its higher aromaticity and stronger solvation capability. The molecular structures in the simulation system were shown in Fig. 1. The molecular structure and corresponding force field parameters were generated using the web-based PolyParGen platform developed at the University of Tokyo (http://polypargen.com/).[33–36] Both bonded and non-bonded interaction parameters required for molecular dynamics simulations were derived from the PolyParGen database. The OPLS-AA force field was adopted to describe intermolecular interactions, where non-bonded terms were represented as the sum of a 12–6 Lennard-Jones potential and a coulombic electrostatic potential.[19,33,37] OPLS-AA provides systematic parameterization for organic molecules and hydrocarbon systems, accurately describing the bonded and non-bonded interactions of the aromatic core, alkyl side chains, and hydroxyl groups in asphaltene molecules.

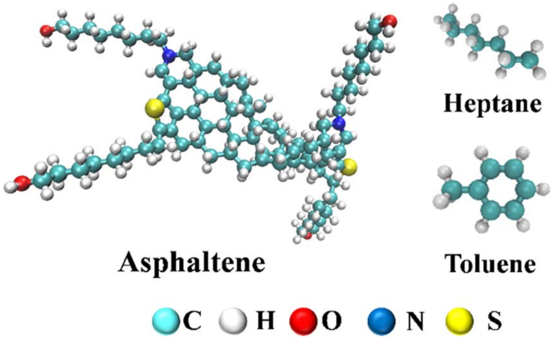

Fig. 1 The molecular structures in the simulation system.

2.2 Simulation system

To systematically investigate the influence of environmental conditions on the aggregation behavior of asphaltene molecules, a one-factor-at-a-time simulation design was employed. The representative island-type asphaltene molecule was selected as the model compound, and three key factors, including solvent composition, temperature, and pressure, were individually examined. The classical simulation systems were shown in Fig. S2.

2.2.1 Solvent effect. To evaluate the impact of solvent effect on asphaltene aggregation, a series of *n*-heptane–toluene mixed solvent systems were constructed. Each simulation box consisted of *n*-heptane, toluene, and asphaltene molecules, with toluene mass fractions of 10%, 20%, 30%, 40%, and 50% in the total solvent. This variation in toluene content allows exploration of how increasing solvent polarity regulates asphaltene dispersion and self-assembly behavior. The detailed composition and box dimensions of each system are listed in Table S1.

2.2.2 Temperature. To examine the influence of temperature on asphaltene aggregation, the solvent composition and pressure were kept constant (toluene mass fraction of 30% and ambient pressure). Simulations were performed at different temperatures to reveal the effect of thermal motion on π–π stacking and hydrogen-bonding interactions among asphaltene molecules. The system composition and detailed parameters are presented in Table S2.

2.2.3 Pressure. To investigate the effect of pressure, simulations were conducted under different pressures while maintaining constant solvent composition and temperature (toluene mass fraction of 30%). This set of simulations aims to clarify how variations in system density and solvent capability influence the stability of asphaltene aggregates. The specific composition and box parameters are provided in Table S3.

By comparing these three groups of single-factor simulation systems, the coupled effects of solvent polarity, temperature, and pressure on the aggregation behavior of island-type asphaltenes were systematically elucidated.

2.3 Simulation process

The molecular dynamics simulations consisted of three sequential stages: energy minimization, NVT (constant temperature, constant volume) pre-equilibration, and NPT (constant temperature, constant pressure) production equilibration. The steepest descent method was used to minimize the total potential energy, and the process was terminated when the energy dropped below 1000.0 kJ (mol^{-1} nm^{-1}), ensuring a stable configuration free of steric overlaps. Each system was then equilibrated under the NVT ensemble for 0.05 ns to reach the target temperature using the Berendsen thermostat with a 2.0 ps coupling constant. Subsequently, a 100.0 ns simulation under the NPT ensemble was performed, during which the Berendsen barostat maintained the pressure at 0.1 MPa (or other designated pressures) with a coupling constant of 2.0 ps. The Particle Mesh Ewald (PME) method with a 12.5 Å cutoff was employed for long-range electrostatic interactions, and periodic boundary conditions were applied with a 2.0 fs integration step. System energies and configurations were recorded every 100.0 ps for subsequent analysis of aggregation behavior.

All simulations were conducted on a high-performance computing platform equipped. Specifically, the platform is a parallel node computer cluster with approximately 500 CPU physical cores in total, equipped with six NVIDIA GPU accelerator cards (one GeForce RTX 2080 Ti and five GeForce RTX 3090 Ti). A heterogeneous CPU-GPU acceleration scheme was adopted to enhance computational efficiency: long-range electrostatics were computed on CPUs to maintain precision, while Lennard-Jones and bonded interactions were accelerated on GPU. All MD simulations were performed using the GROMACS 2019 package. This hybrid architecture substantially improved computational performance and stability, ensuring accurate and efficient simulation of the complex asphaltene systems.

3. Results and discussions

3.1 Equilibrium analysis of the simulation systems

The equilibrium state of each simulation system was evaluated by monitoring the variation of total energy with simulation time. The time evolution curves of total energy under different environmental conditions are shown in Fig. 2. It can be observed that after entering the NPT stage, the total energy of all systems rapidly decreased and subsequently stabilized, indicating that atomic interactions, temperature, and pressure had equilibrated within the target ranges. This confirms that all systems reached a dynamic equilibrium suitable for further structural and energetic analysis.

When comparing systems with different toluene mass fractions, the total energy gradually increased with higher toluene content. The system with 10% toluene exhibited the lowest energy, whereas the one with 50% toluene showed the highest, with an overall variation of ~10 000 kJ mol^{-1}. This trend suggests that as toluene, a good solvent for asphaltenes,

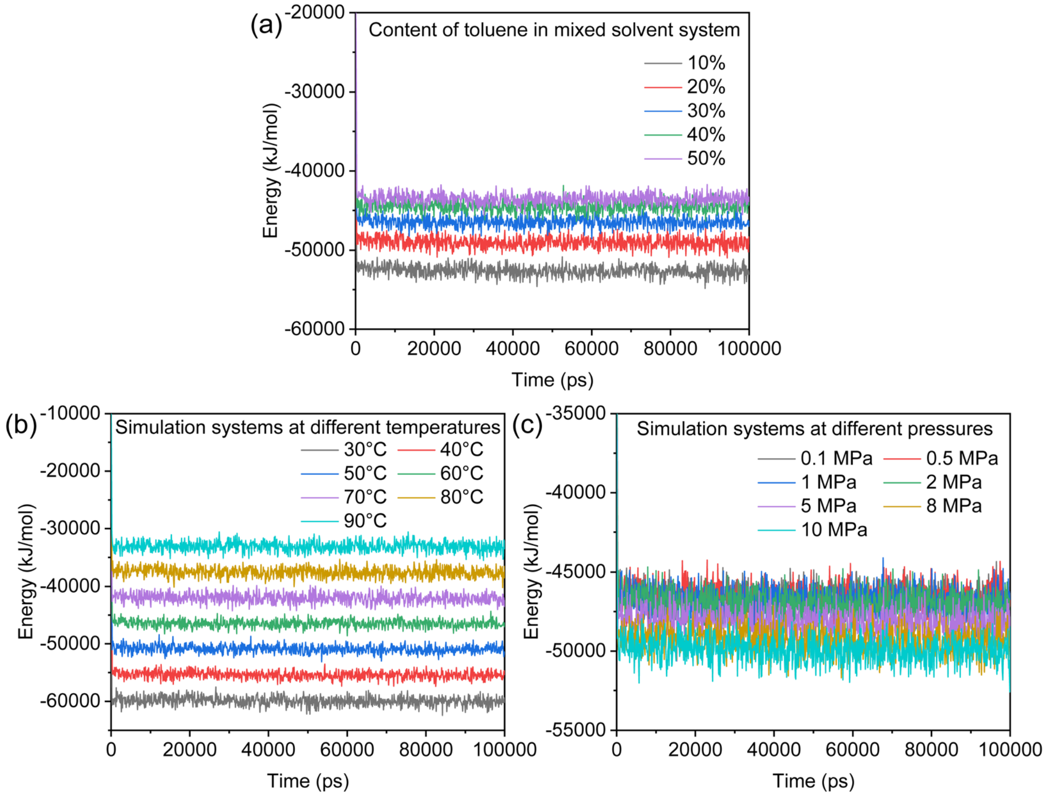

Fig. 2 The variation of total energy of the simulation system over time: (a) different toluene content systems; (b) different temperature systems; (c) different pressure systems.

becomes more dominant, the intermolecular aggregation among asphaltene molecules is weakened, leading to higher system energy and reduced aggregate stability. Under different temperature conditions, the total energy increased notably with rising temperature, and its fluctuations became more pronounced. The system exhibited the lowest energy at 30 °C and the highest at 90 °C, with a variation of approximately 30 000 kJ mol^{-1}. This behavior results from intensified molecular motion at elevated temperatures, where increased kinetic energy of asphaltene, toluene, and *n*-heptane molecules raises the overall system energy. In contrast, changes in pressure exerted a smaller effect: as the pressure increased from 0.1 MPa to 10 MPa, the total energy slightly decreased, with a variation of ~5000 kJ mol^{-1}. Higher pressure compresses intermolecular distances and enhances interaction strength, improving thermodynamic stability, though its influence remains weaker than that of temperature or solvent composition. The energy evolution curves confirm that all systems achieved equilibrium, and the results demonstrate that solvent polarity and temperature are the dominant factors controlling system energy and stability, whereas pressure exerts only a secondary effect.

3.2 Effect of solvent composition on asphaltene aggregation

3.2.1 Molecular energy. The molecular energy of asphaltene reflects its thermodynamic characteristics and stability under different solvent environments. As shown in Fig. 3a, the total energy of asphaltene molecules in systems with varying toluene contents decreases gradually over the course of the simulation and eventually stabilizes, indicating that thermodynamic equilibrium was achieved in all cases. However, the rate and magnitude of energy variation strongly depend on toluene concentration. At low toluene fractions (10%, 20%, and 30%), the total energy decreases more rapidly and significantly, suggesting that the system becomes more stable and that the aggregation tendency of asphaltene molecules is enhanced. In contrast, at high toluene fractions (40% and 50%), the decrease in total energy is much smaller and slower, implying weaker intermolecular attractions and a more dispersed molecular state. Particularly, in the 10% toluene system, the total energy drops sharply in the early stage of the simulation, reflecting fast formation of nanoaggregates, whereas in the 50% toluene system, the decline is moderate, indicating that higher toluene content suppresses aggregation. This observation is consistent with the dynamic aggregation behavior discussed later.

van der Waals and electrostatic interaction energies are the two principal components of the total molecular energy, as illustrated in Fig. 3b and c. The variation of van der Waals energy closely follows the trend of the total energy: at low toluene contents, the van der Waals energy decreases rapidly and substantially, indicating strong intermolecular attractions that promote aggregation; at high toluene contents, the decline is slower and less pronounced, suggesting weakened interactions and hindered aggregation. The electrostatic energy, by contrast, fluctuates more significantly across systems but

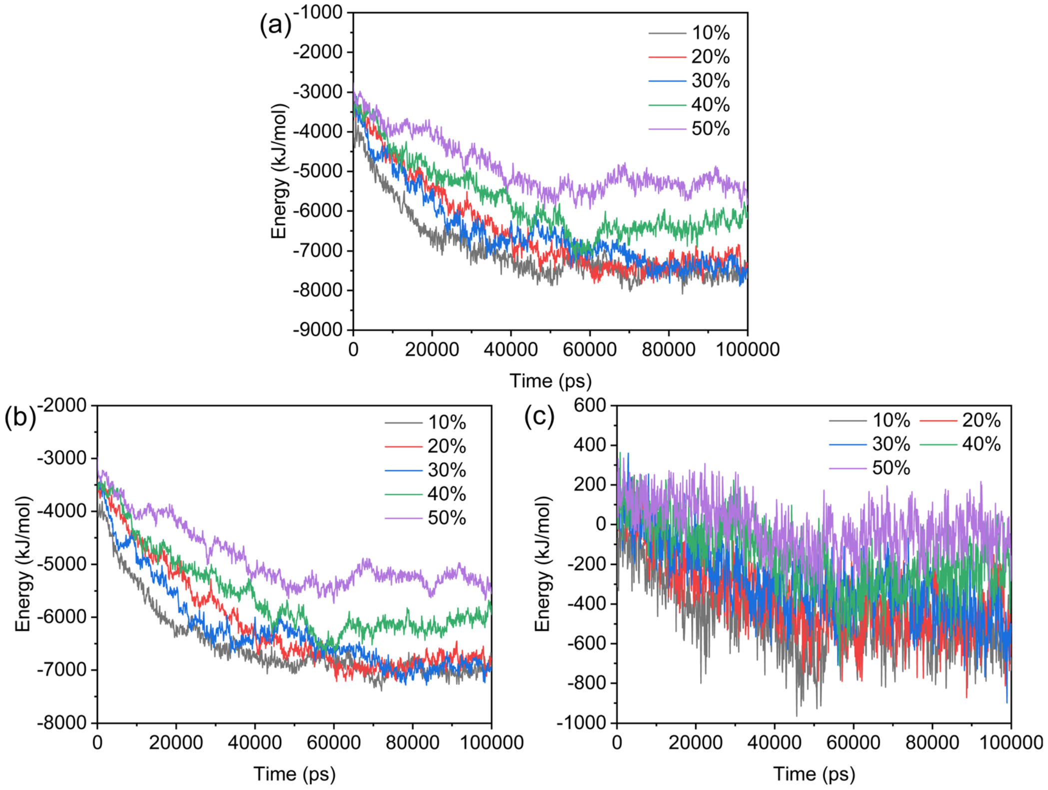

Fig. 3 Time-dependent energy curves of asphaltene molecules in simulation systems with different toluene contents: (a) total energy; (b) van der Waals interaction energy; (c) electrostatic interaction energy.

generally shows a gradual decrease. At lower toluene contents, electrostatic interactions exhibit weak attraction and contribute slightly to aggregation, whereas at higher toluene contents, the electrostatic energy fluctuates around zero, implying negligible influence. Overall, van der Waals forces dominate the aggregation process of asphaltene molecules, contributing far more than electrostatic interactions. Both total energy and van der Waals energy decrease over time, indicating progressive thermodynamic stabilization. Systems with low toluene fractions (≤30%) show a greater energy decline and stronger aggregation tendency, forming compact asphaltene clusters, while systems with high toluene fractions (≥40%) exhibit smaller energy changes and a more dispersed molecular configuration, indicating inhibited aggregation.

3.2.2 SASA. The SASA of asphaltene molecules serves as an indicator of molecular exposure and aggregation compactness in different solvent environments. A larger SASA indicates a more open molecular structure with greater solvent exposure, whereas a smaller SASA indicates a more compact structure or aggregation with other molecules, reducing the solvent-accessible area. As shown by the time evolution of SASA, all systems exhibited a gradual decrease in SASA values followed by stabilization, indicating the formation of energetically stable aggregates. In systems with low toluene content (10 to 30%), the SASA values declined sharply and stabilized at relatively low levels, implying the formation of dense and compact aggregates (Fig. 4a). In contrast, at higher toluene contents (40 to 50%), the SASA decreased more slowly and showed slight fluctuations at later stages, suggesting weakened intermolecular attractions and partial disaggregation of asphaltene clusters (Fig. 4b). The average SASA values in the final 1 ns of simulation further confirm these trends (Fig. 4c). At low toluene concentrations (10 to 30%), asphaltene molecules exhibited average SASA values around 210 nm^2, indicating tight aggregation structures. In high-toluene systems (40 to 50%), SASA increased significantly to approximately 270 to 290 nm^2, reflecting stronger solvation effects that reduce van der Waals and π–π stacking interactions between asphaltene molecules, leading to more dispersed and less compact configurations. Overall, the SASA analysis demonstrates that increasing toluene concentration effectively suppresses molecular aggregation and enhances the dispersion of asphaltene molecules within the solvent environment.

3.2.3 Number of intermolecular hydrogen bonds. The hydroxyl groups on the asphaltene molecular side chains can form intermolecular hydrogen bonds, which serve as an important driving force for aggregation. Hydrogen bonds were identified using classical geometric criteria applied to each frame of the simulation trajectory, with a donor–acceptor distance (D–A) ≤ 0.35 nm, a hydrogen–acceptor distance (H–A) ≤ 0.25 nm, and a donor–hydrogen–acceptor angle (∠D–H–A) ≥ 120°. As shown in Fig. 4d, the number of hydrogen bonds in all systems increases over time and stabilizes at later stages, indicating that equilibrium was achieved. At low toluene concentrations (10 to 30%), the hydrogen bond number is higher and grows faster, for example, in the 10% toluene system, it rises from ~10 to 24, suggesting that low toluene content facilitates hydrogen bonding and promotes aggregation. In contrast, at higher toluene levels (40 to 50%), the hydrogen bond number is markedly lower (increasing only from ~4 to 9), implying that the solvation effect of toluene weakens hydroxyl–hydroxyl

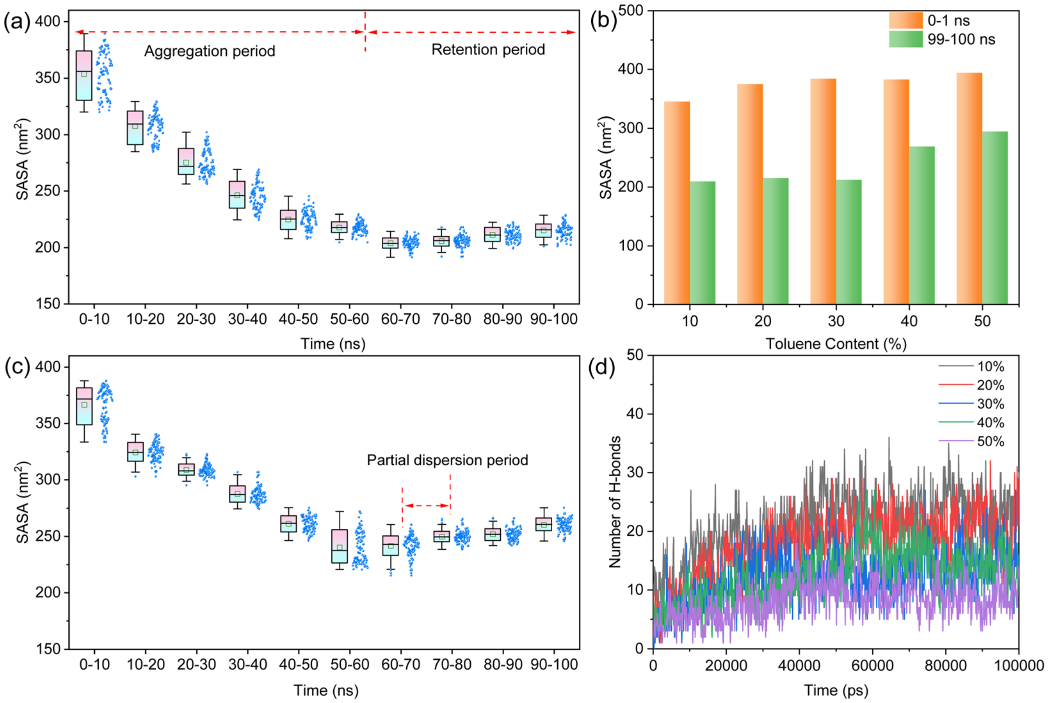

Fig. 4 (a) The distribution of SASA in the 20% toluene content simulation system; (b) the distribution of SASA in the 40% toluene content simulation system; (c) comparison of the average SASA in simulation systems; (d) the variation curve of the number of hydrogen bonds.

interactions and suppresses aggregate formation. Overall, higher toluene concentrations reduce hydrogen bonding and enhance molecular dispersion, whereas lower toluene contents strengthen hydrogen-bond interactions and favor the formation of compact asphaltene aggregates.

3.3 Effect of temperature on asphaltene aggregation

3.3.1 Molecular energy. Temperature plays a crucial role in determining the energy distribution and aggregation behavior of molecular systems. As shown in Fig. 5a, the total energy of asphaltene molecules decreases progressively over time under all temperature conditions and eventually stabilizes, indicating the attainment of dynamic equilibrium. During the initial stage (0 to 20 ns), the rapid energy drop reflects strong intermolecular attractions driving the aggregation process. In the intermediate stage (20 to 50 ns), the energy decline slows as the system undergoes structural rearrangement, and in the final stage, the energy approaches a stable plateau. Among all conditions, the systems at moderate temperatures (60 to 70 °C) exhibit the lowest total energy and the most stable aggregates, while low-temperature systems (30 to 50 °C) display slightly higher energy due to limited molecular motion, and high-temperature systems (80 to 90 °C) show elevated energy levels caused by intensified thermal motion that disrupts aggregation stability. A brief energy increase observed around 30 to 35 ns in the medium- and high-temperature systems suggests a transient imbalance between thermal agitation and intermolecular attraction. At these stages, enhanced molecular motion allows some asphaltene molecules to partially detach from aggregates, leading to temporary energy elevation. Subsequent reorganization and re-stacking restore system stability, reflected by the subsequent energy decline. This transient behavior highlights that higher temperatures intensify the competition between aggregation forces and thermal motion, affecting the stability and morphology of aggregates. As depicted in Fig. 5b, the variation of van der Waals interaction energy closely parallels that of the total energy, both showing a rapid decline followed by stabilization, confirming that van der Waals forces dominate the aggregation process. Minor fluctuations at medium and high temperatures correspond to temporary disassembly and rearrangement of molecular clusters. In contrast, electrostatic interaction energy varies little across temperatures, indicating its limited contribution (Fig. 5c). The aggregation of asphaltene molecules is therefore primarily driven by van der Waals and π–π stacking interactions. Comparison of the final equilibrium energies shows that the systems at 60 to 70 °C achieve the lowest total energy, indicating optimal thermodynamic stability, while both low and high temperatures are less favorable for stable aggregate formation due to insufficient or excessive molecular motion.

3.3.2 SASA. The solvent accessible surface area (SASA) of asphaltene molecules reflects the compactness and packing characteristics of molecular aggregates. As shown in Fig. 6a, SASA values at all temperatures exhibit a general trend of rapid

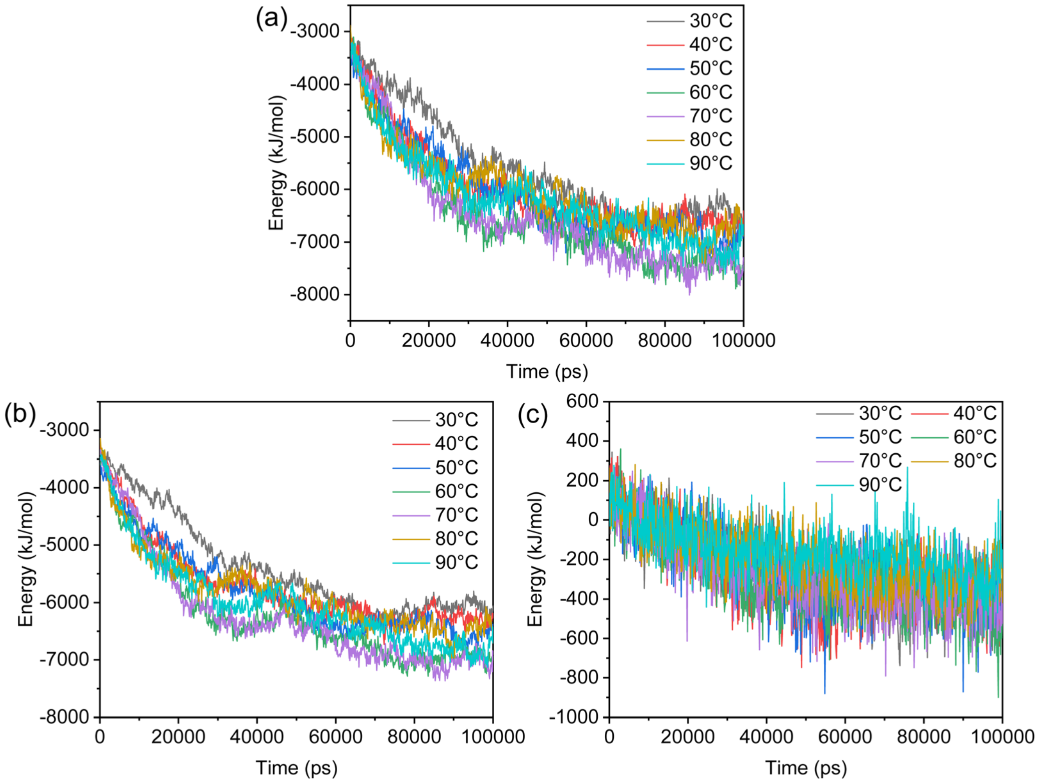

Fig. 5 Time-dependent energy curves of asphaltene molecules in simulation systems with different temperatures: (a) total energy; (b) van der Waals interaction energy; (c) electrostatic interaction energy.

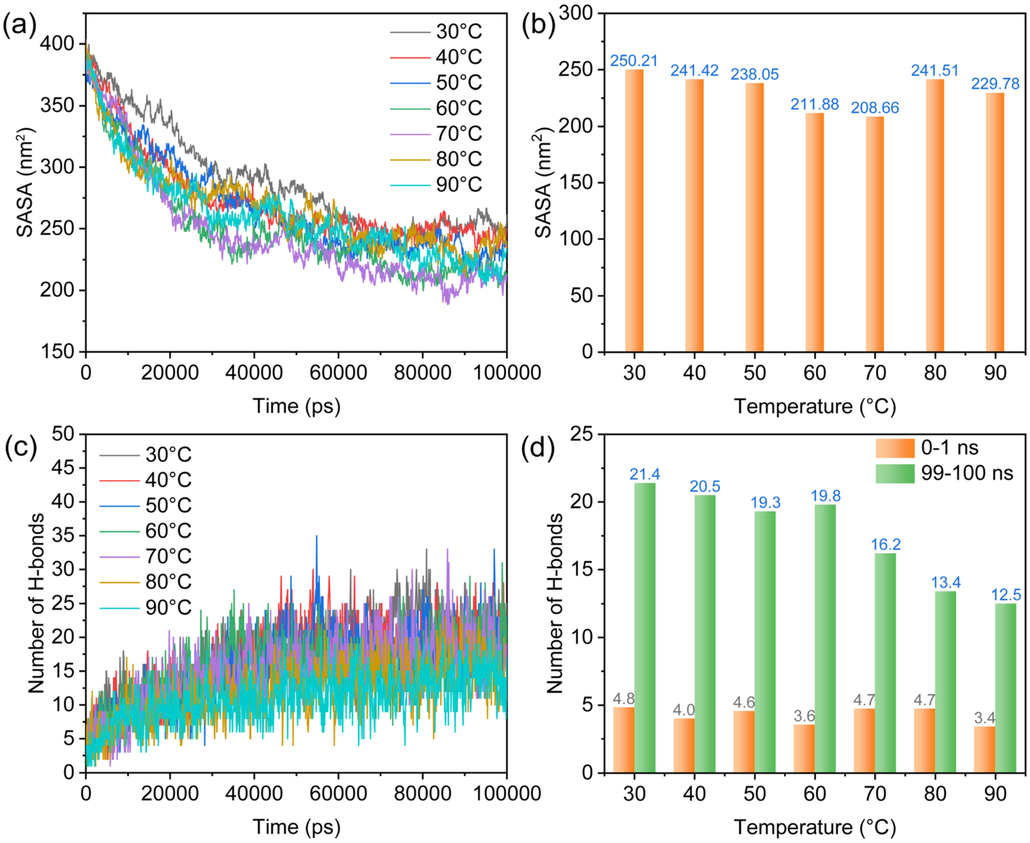

Fig. 6 (a) The variation curve of SASA in simulation systems with different temperatures; (b) comparison of the average SASA in simulation systems; (c) the variation curve of number of hydrogen bonds in simulation systems with different temperatures; (d) comparison of the average number of hydrogen bonds.

initial decrease, followed by minor fluctuations and eventual stabilization, indicating the progressive formation of stable aggregates. At low temperature (30 °C), SASA decreases quickly within 60 ns and stabilizes thereafter, suggesting early aggregation and dense cluster formation. At moderate temperature (70 °C), SASA shows a brief increase after an initial drop and then decreases again to a stable level, implying that asphaltene molecules undergo partial dispersion and structural reconfiguration before forming compact, thermodynamically stable aggregates. In contrast, at high temperature (90 °C), SASA exhibits larger fluctuations and a higher final value, indicating looser aggregation and enhanced molecular mobility that promotes partial disassembly and rearrangement of aggregates.

The average SASA values during the equilibrium stage (Fig. 6b) show a nonlinear temperature dependence. The lowest SASA values (~210 nm^2) occur at moderate temperatures (60 to 70 °C), corresponding to the most compact aggregates. Slightly higher SASA values are observed at low temperatures (30 to 50 °C), while further increases at high temperatures (~230 to 240 nm^2) reflect the destabilization of aggregates due to intensified thermal motion. These results confirm that moderate temperatures favor the formation of dense and stable asphaltene aggregates, whereas both low and high temperatures reduce aggregate compactness and stability.

3.3.3 Number of intermolecular hydrogen bonds. The evolution of intermolecular hydrogen bonds among asphaltene molecules under different temperature conditions is shown in Fig. 6c. The number of hydrogen bonds increases with simulation time and eventually stabilizes at later stages, indicating that as molecular separation decreases and aggregation proceeds, hydrogen-bond interactions between asphaltene molecules gradually strengthen. The initially low hydrogen bond count rises steadily as aggregation develops, confirming that hydrogen bonding contributes to the energetic stabilization of the aggregates. Distinct differences are observed in the final number of hydrogen bonds across temperature conditions (Fig. 6d). At low temperatures (30 to 50 °C), more hydrogen bonds are formed, suggesting that weaker thermal motion facilitates hydrogen bond formation and retention. In contrast, at higher temperatures (80 to 90 °C), the hydrogen bond number decreases significantly, as intensified thermal motion disrupts hydrogen bonding, leading to easier bond breaking and rearrangement. Overall, the number of hydrogen bonds declines with increasing temperature, demonstrating that elevated temperatures weaken the contribution of hydrogen bonding to asphaltene aggregation, whereas low and moderate temperatures favor the formation of stable hydrogen-bond networks and compact aggregates.

3.4 Effect of pressure on asphaltene aggregation

3.4.1 Molecular energy. The influence of pressure on molecular energy distribution primarily arises from changes in intermolecular interactions and solvent compression effects. As pressure increases, system compression enhances potential and kinetic interactions, whereas at lower pressures, system expansion weakens them. As shown in Fig. 7a, the total energy of asphaltene molecules decreases with simulation time and stabilizes under all pressure conditions, indicating that molecular aggregation and dynamic equilibrium are achieved across the simulations. Pressure exerts a relatively minor effect compared to solvent composition or temperature. At low pressures (0.1 to 1 MPa), energy curves nearly overlap, while at 2 MPa, a pronounced fluctuation and the highest final energy suggest poorer thermodynamic stability of the aggregates. When pressure increases further to 5 to 10 MPa, energy fluctuations diminish and total energy slightly decreases, implying that higher pressure enhances intermolecular attraction and leads to more compact aggregation.

The variations in van der Waals and electrostatic interaction energies under different pressures are shown in Fig. 7b and c. The van der Waals energy follows the same trend as the total energy, confirming that aggregation is primarily driven by van der Waals forces. Increasing pressure reduces intermolecular distances, strengthens van der Waals attraction, and promotes denser packing of asphaltene molecules, thereby lowering the total energy. In contrast, electrostatic interaction energy changes little with pressure, indicating its limited contribution to aggregation. Comparative analysis shows that the final average total energy of asphaltene molecules is lowest at 0.1 MPa (−7540 kJ mol^{-1}), representing the most stable aggregate, while the highest energy occurs at 2 MPa (−6346 kJ mol^{-1}), corresponding to a looser structure. Beyond 2 MPa, total energy gradually decreases with increasing pressure, and aggregates become denser. These results demonstrate that pressure affects asphaltene aggregation primarily by modulating solvent compression and intermolecular forces, with moderate to high pressures favoring more compact and stable aggregate formation.

3.4.2 SASA. The solvent accessible surface area (SASA) of asphaltene molecules under different pressures is shown in Fig. 8a and b, exhibiting a distinct nonlinear dependence on pressure. The system at moderate pressure (2 MPa) displays the highest SASA value (253.15 nm^2), indicating enhanced molecular solvation, a looser aggregate structure, and lower overall stability. In contrast, both low-pressure (0.1 MPa) and high-pressure (10 MPa) systems show the lowest SASA values (211.88 and 212.52 nm^2, respectively), reflecting the formation of dense and stable aggregates. At low pressures (≤2 MPa), increasing pressure enhances solvent compression, allowing toluene molecules to penetrate the asphaltene clusters more effectively and increase the solvent-accessible area. Beyond 2 MPa, further compression affects both solvent and asphaltene molecules, inducing side-chain folding and restricting

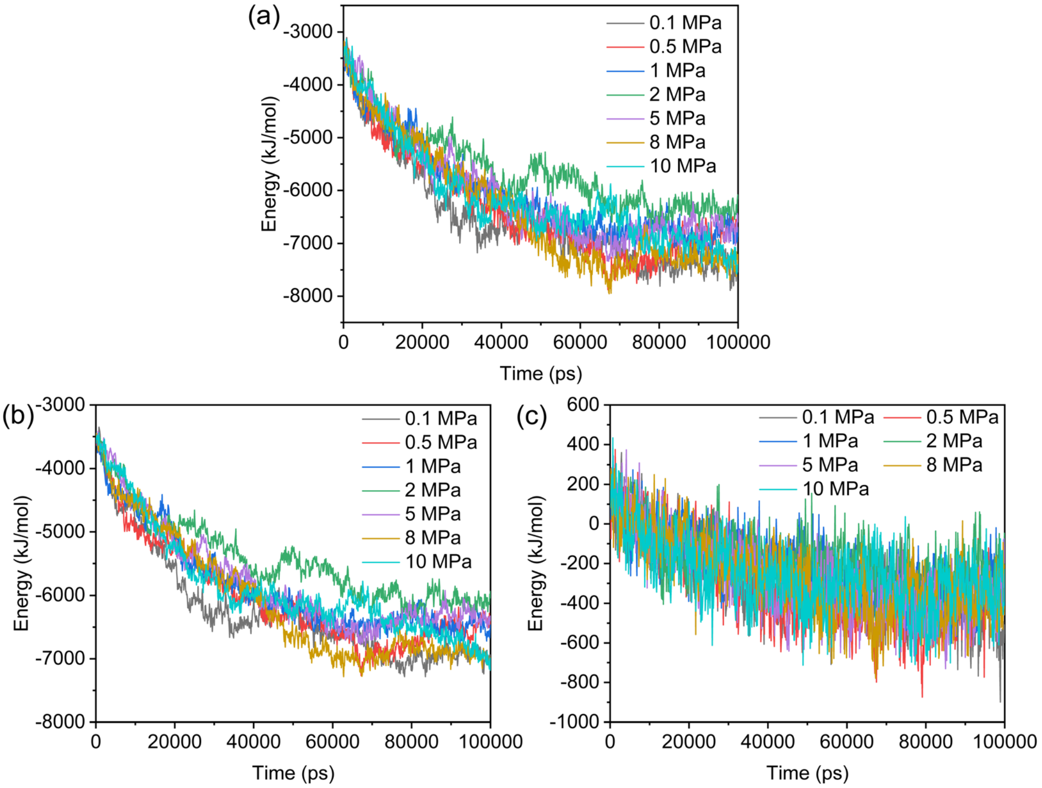

Fig. 7 Time-dependent energy curves of asphaltene molecules in simulation systems with different pressures: (a) total energy; (b) van der Waals interaction energy; (c) electrostatic interaction energy.

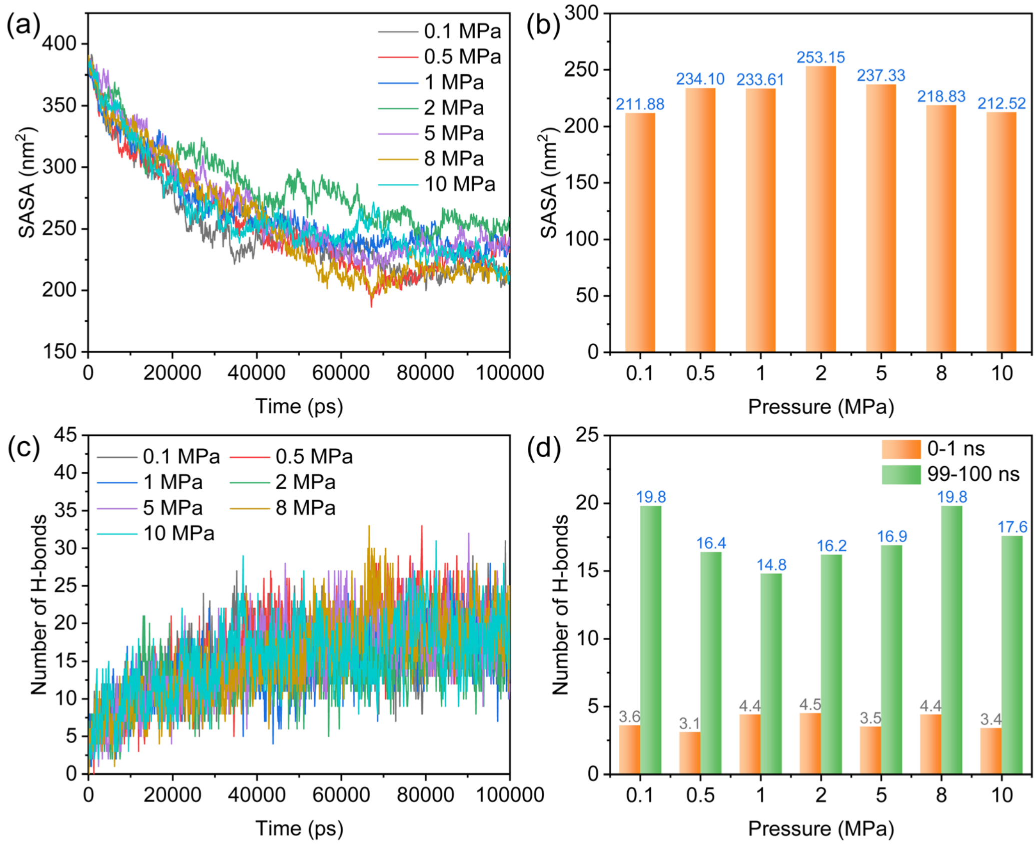

Fig. 8 (a) The variation curve of SASA in simulation systems with different pressures; (b) comparison of the average SASA in simulation systems; (c) the variation curve of number of hydrogen bonds in simulation systems with different pressures; (d) comparison of the average number of hydrogen bonds.

molecular motion, which leads to reduced SASA. Therefore, pressure modulates not only the solvation behavior of asphaltene during aggregation but also the final compactness of the aggregates: moderate pressures (~2 MPa) promote dispersion, whereas low and high pressures favor the formation of denser, more stable asphaltene clusters.

3.4.3 Number of intermolecular hydrogen bonds. The evolution of intermolecular hydrogen bonds among asphaltene molecules under different pressures is illustrated in Fig. 8c. In all pressure systems, the number of hydrogen bonds increases over time and stabilizes at later stages, indicating that as molecular aggregation proceeds, hydrogen bonding interactions become stronger and reach dynamic equilibrium. The growth trends of hydrogen bonds are largely consistent across pressures, suggesting that pressure has only a minor influence on their formation process. A comparison of final hydrogen bond numbers reveals a nonlinear relationship with pressure: higher bond counts (~19.8) occur at 0.1 MPa and 8 MPa, while the lowest (~14.8) appears at 1 MPa (Fig. 8d). This variation likely arises from the random effects of pressure on asphaltene side-chain conformations, which alter the spatial orientation and contact probability of hydroxyl groups, leading to stochastic hydrogen bond formation. Overall, the impact of pressure on hydrogen bonding is non-monotonic, indirectly modulating bond formation and stability by influencing molecular conformation and steric hindrance.

Above all, Fig. S3 concisely summarizes three typical conditions that promote the formation of compact asphaltene clusters: low toluene fraction (≤30%), moderate temperature (*ca.* 60–70 °C), and either excessively low or excessively high pressure (deviating from the moderate pressure range around ~2 MPa). Under low toluene fraction, van der Waals attraction is enhanced and SASA decreases, leading to compact aggregation; at moderate temperature, the total energy reaches its minimum, van der Waals forces are strongest, and the hydrogen-bond network is ordered, resulting in the most stable and compact aggregates; at pressures that are too low or too high, both total energy and SASA decrease, yielding denser structures, whereas at moderate pressure (~2 MPa) the aggregates become looser. These observations are fully consistent with the SASA and hydrogen bond analyses and the nonlinear effects of temperature and pressure.

4. Conclusions

The aggregation behavior of asphaltene molecules critically affects crude oil stability, flowability, and reservoir plugging risks. A molecular-level understanding of their structural evolution under varying environmental conditions is therefore essential for efficient petroleum production and flow assurance. In this work, the representative "island" asphaltene molecule asphaltene was investigated using molecular dynamics simulations to elucidate the effects of solvent composition, temperature, and pressure on its aggregation behavior. The analysis focused on molecular energy, solvent accessible surface area (SASA), and intermolecular hydrogen bonding to reveal the thermodynamic characteristics and structural evolution of asphaltene aggregates.

The results demonstrate that solvent composition exerts a dominant influence on asphaltene aggregation. Increasing toluene content weakens van der Waals attractions, reduces energy decline, and promotes molecular dispersion, whereas low toluene fractions (≤30%) enhance aggregation and lead to compact clusters. van der Waals interactions are identified as the primary driving force, while SASA and hydrogen bond analyses confirm that higher toluene contents enhance solvation and inhibit aggregation.

Temperature exhibits a distinct nonlinear effect on asphaltene aggregation. At moderate temperatures (60 to 70 °C), the total energy reaches its minimum, van der Waals forces are strongest, and the aggregates are most stable and compact. Low temperatures restrict molecular motion and hinder optimal stacking, while high temperatures increase thermal motion, leading to partial disaggregation. Both SASA and hydrogen bond trends indicate that moderate temperatures are most favorable for stable aggregate formation.

Pressure has a relatively minor but non-negligible influence. At moderate pressure (~2 MPa), total energy and SASA reach their highest values, corresponding to looser aggregates and stronger solvation effects. At low and high pressures, both energy and SASA decrease, resulting in denser and more stable structures. The number of hydrogen bonds varies nonlinearly with pressure, reflecting the stochastic influence of pressure on side-chain conformations and solvent compression effects.

In summary, the aggregation of asphaltene molecules is governed by the synergistic effects of solvent polarity, temperature, and pressure: solvent composition acts as the dominant factor, temperature as the regulating factor, and pressure as the secondary stabilizing factor. Moderate polarity and mid-range temperature and pressure conditions favor the formation of thermodynamically stable, compact aggregates. This study provides molecular-level insights into the aggregation mechanisms of asphaltenes, offering a theoretical basis for predicting and mitigating asphaltene deposition in reservoirs and guiding the design of stabilizing additives for complex crude oil systems.

Author contributions

Cun Hu: conceptualization, data curation, formal analysis, funding acquisition, investigation, methodology, resources, software, supervision, validation, visualization, writing – review & editing. Dandan Hong: data curation, formal analysis, investigation, writing – original draft. E. Fu: investigation, software, visualization, writing – original draft. Yalou Sun: investigation, software, visualization. Jipeng Wang: methodology, software, visualization. Li Chen: investigation, software, visualization. Xiaoyu Hu: methodology, software, visualization. Jun Wang: investigation, software, visualization. Zhaohui Hu: methodology, software, visualization. Wenjing Shi: investigation, software, visualization. Zhi Cao: methodology, software, visualization. Changchun Wang: investigation, software, visualization. Lulu Hu: conceptualization, funding acquisition, methodology, project administration, resources, supervision, writing – review & editing.

Conflicts of interest

The authors declare that they have no known competing financial interests or personal relationships that could have appeared to influence the work reported in this paper.

Data availability

The authors confirm that the data supporting the findings of this study are available within the article and its supplementary materials (SI). Supplementary information is available. See DOI: https://doi.org/10.1039/d6ra00135a.

Acknowledgements

This work was supported by Science and Technology Program of Gansu Province (25JRRA418, 25RCKA037, 26YFGA014), Talent Project of Gansu Province (2025QNGR50) and Independent Scientific Research Fund of the 404 Company Limited (2024-1141).

References

1 K. Primerano, J. Mirwald and B. Hofko, Asphaltenes and maltenes in crude oil and bitumen: A comprehensive review of properties, separation methods, and insights into structure, reactivity and aging, *Fuel*, 2024, **368**, 131616.

2 X. Liu, H. Zhu, S. Li, Y. Gao, H. Wang, Y. Zhou, H. Peng, Y. Lei and P. Yu, Effect of temperature on the aggregation kinetic and interaction mode of asphaltene in Toluene-Heptane system at molecular level using molecular dynamics (MD) simulation, *J. Mol. Liq.*, 2023, **384**, 122167.

3 B. Busahmin and B. Maini, A Potential Parameter for A Non-Darcy Form of Two-Phase Flow Behaviour, Compressibility Related, *Int. J. Eng. Technol.*, 2018, **7**, 126–131.

4 W. Pu, M. He, X. Yang, R. Liu and C. Shen, Experimental study on the key influencing factors of phase inversion and stability of heavy oil emulsion: Asphaltene, resin and petroleum acid, *Fuel*, 2022, **311**, 122631.

5 P. Zuo, S. Qu and W. Shen, Asphaltenes: Separations, structural analysis and applications, *J. Energy Chem.*, 2019, **34**, 186–207.

6 B. Peng, L. Yuan, X. Tang, Y. Wang, Y. Li, W. Liu and Y. Pei, Molecular dynamics simulations of aggregation and viscosity properties of model asphaltene molecules containing a polycyclic hydrocarbon nucleus with toluene

additive under shear interactions, *RSC Adv.*, 2024, **14**, 2577–2589.

7 A. Khormali, A. R. Sharifov and D. I. Torba, Experimental and modeling study of asphaltene adsorption onto the reservoir rocks, *Pet. Sci. Technol.*, 2018, **36**, 1482–1489.

8 Y. Peng, X. Zhang, L. Cheng, H. Zhang, J. Tang, H. Chen, Q. Fan and X. Ouyang, Effect of Asphaltenes on the Stability of Water in Crude Oil Emulsions, *Materials*, 2025, **18**, 630.

9 P. Yu, Y. Zhou, S. Zeng, D. Lai, H. Zhu, S. Yang, H. Peng and Y. Lei, Microscopic mechanism of single-walled carbon nanotubes (SWCNTS) as a dispersant for alleviating asphaltene aggregation, *Colloids Surf., A*, 2024, **690**, 133810.

10 M. V. Dastjerdi, H. Sayahi, A. Koochaki and Z. Jamshidi, Asphaltene aggregation under the influence of structural features and interaction energies: Combination of quantum mechanical and molecular dynamics approaches, *Colloids Surf., A*, 2023, **671**, 131660.

11 D. Simionesie, G. O'Callaghan, J. L. L. F. S. Costa, L. Giusti, W. J. Kerr, J. Sefcik, P. A. Mulheran and Z. J. Zhang, Clustering behaviour of polyaromatic compounds mimicking natural asphaltenes, *Colloids Surf., A*, 2020, **603**, 125221.

12 S. Fakher, A. Al-Sakkaf and M. Ali, Evaluating key parameters impacting asphaltene permeability reduction behavior in micro-pores during carbon dioxide injection, *Fuel*, 2023, **339**, 126933.

13 Y. Zhang, Q. Lin, A. Q. Raeini, Y. Onaka, H. Iwama, K. Takabayashi, M. J. Blunt and B. Bijeljic, Pore-scale imaging of asphaltene deposition with permeability reduction and wettability alteration, *Fuel*, 2022, **316**, 123202.

14 S. Yuan, L. Wang, X. Zhang, X. Cao and S. Yuan, Molecular structure-dependent interfacial behavior of asphaltenes at the oil-water interface, *Colloids Surf., A*, 2026, **733**, 139296.

15 G. Lv, F. Gao, G. Liu and S. Yuan, The properties of asphaltene at the oil-water interface: A molecular dynamics simulation, *Colloids Surf., A*, 2017, **515**, 34–40.

16 M. L. Chacón-Patiño, S. M. Rowland and R. P. Rodgers, Advances in Asphaltene Petroleomics. Part 3. Dominance of Island or Archipelago Structural Motif Is Sample Dependent, *Energy Fuels*, 2018, **32**, 9106–9120.

17 F. Alvarez-Ramírez and Y. Ruiz-Morales, Island versus Archipelago Architecture for Asphaltenes: Polycyclic Aromatic Hydrocarbon Dimer Theoretical Studies, *Energy Fuels*, 2013, **27**, 1791–1808.

18 H. Groenzin and O. C. Mullins, Molecular Size and Structure of Asphaltenes from Various Sources, *Energy Fuels*, 2000, **14**, 677–684.

19 C. Wang, P. Liu, J. Zhao, J. Hu, J. Du, X. Chen, X. Song, G. Wang, J. Liu and L. He, Topological isomerism governs asphaltene aggregation: A mechanistic study combining molecular dynamics and experiments, *Fuel*, 2025, **385**, 134165.

20 H. Sabbah, A. L. Morrow, A. E. Pomerantz and R. N. Zare, Evidence for Island Structures as the Dominant Architecture of Asphaltenes, *Energy Fuels*, 2011, **25**, 1597–1604.

21 A. Neumann, M. L. Chacón-Patiño, R. P. Rodgers, C. P. Rüger and R. Zimmermann, Investigation of Island/Single-Core- and Archipelago/Multicore-Enriched Asphaltenes and Their Solubility Fractions by Thermal Analysis Coupled with High-Resolution Fourier Transform Ion Cyclotron Resonance Mass Spectrometry, *Energy Fuels*, 2021, **35**, 3808–3824.

22 O. P. Strausz, P. a. Peng and J. Murgich, About the Colloidal Nature of Asphaltenes and the MW of Covalent Monomeric Units, *Energy Fuels*, 2002, **16**, 809–822.

23 B. Schuler, G. Meyer, D. Peña, O. C. Mullins and L. Gross, Unraveling the Molecular Structures of Asphaltenes by Atomic Force Microscopy, *J. Am. Chem. Soc.*, 2015, **137**, 9870–9876.

24 B. Schuler, S. Fatayer, G. Meyer, E. Rogel, M. Moir, Y. Zhang, M. R. Harper, A. E. Pomerantz, K. D. Bake, M. Witt, D. Peña, J. D. Kushnerick, O. C. Mullins, C. Ovalles, F. G. A. van den Berg and L. Gross, Heavy Oil Based Mixtures of Different Origins and Treatments Studied by Atomic Force Microscopy, *Energy Fuels*, 2017, **31**, 6856–6861.

25 S. Kananpanah, M. Bayat, M. A. Mousavian and A. R. Solaimany Nazar, Impacts of physico-chemical properties of asphaltene aggregates on optimization of the thermal de-asphaltene process, *J. Petrol. Sci. Eng.*, 2016, **147**, 718–725.

26 S. Tazikeh, O. Mohammadzadeh and S. Zendehboudi, Characterization and multiphase flow of Oil/CO_2 systems in porous media focusing on asphaltene precipitation: A systematic review, *Geoenergy Sci. Eng.*, 2025, **247**, 213554.

27 A. Eftekhari, J. S. Amin and S. Zendehboudi, A molecular dynamics approach to investigate effect of pressure on asphaltene self-aggregation, *J. Mol. Liq.*, 2023, **376**, 121347.

28 F. Perez, A. Striolo, J. Wang, J. Patterson and R. Kini, Molecular Signatures of Asphaltene Precipitation in a Depressurization Process, *Energy Fuels*, 2023, **37**, 14688–14698.

29 N. B. Ismail and B. Hascakir, Impact of asphaltenes and clay interaction on in-situ combustion performance, *Fuel*, 2020, **268**, 117358.

30 Z.-x. Dong, J. Wang, G. Liu, M.-q. Lin and M.-y. Li, Experimental study on asphaltene precipitation induced by CO_2 flooding, *Pet. Sci.*, 2014, **11**, 174–180.

31 S. Zhang, L. Zhang, X. Lu, C. Shi, T. Tang, X. Wang, Q. Huang and H. Zeng, Adsorption kinetics of asphaltenes at oil/water interface: Effects of concentration and temperature, *Fuel*, 2018, **212**, 387–394.

32 D. Wang, D. Yang, C. Huang, Y. Huang, D. Yang, H. Zhang, Q. Liu, T. Tang, M. Gamal El-Din, T. Kemppi, B. Perdicakis and H. Zeng, Stabilization mechanism and chemical demulsification of water-in-oil and oil-in-water emulsions in petroleum industry: A review, *Fuel*, 2021, **286**, 119390.

33 C. Wang, P. Liu, J. Zhao, J. Du, X. Chen, X. Wu, X. Song, G. Wang, J. Liu and Y. Xiao, Topological isomerism design of Demulsifiers: A fusion of molecular dynamics simulation and experiment, *J. Mol. Liq.*, 2024, **404**, 125000.

34 W. L. Jorgensen and J. Tirado-Rives, Molecular modeling of organic and biomolecular systems using BOSS and MCPRO, *J. Comput. Chem.*, 2005, **26**, 1689–1700.

35 J. Wang, W. Wang, P. A. Kollman and D. A. Case, Automatic atom type and bond type perception in molecular mechanical calculations, *J. Mol. Graphics Modell.*, 2006, **25**, 247–260.

36 M. Yabe, K. Mori, K. Ueda and M. Takeda, Development of PolyParGen Software to Facilitate the Determination of Molecular Dynamics Simulation Parameters for Polymers, *J. Comput. Chem., Jpn.*, 2019, **5**, DOI: 10.2477/jccjie.2018-0034.

37 X. Song, S. Wang, X. Duan, H. Liu, S. Chen, T. Long, X. Xu, J. Tang, T. Li, S. Zhao and H. Liu, Structural heterogeneity effects on microgel deswelling and interfacial properties: An extensive computational study, *Appl. Surf. Sci.*, 2022, **605**, 154639.